Photoinduced Electron Transfer and Nonlinear Absorption in Poly(carbazole-alt-2,7-fluorene)s Bearing Perylene Diimides as Pendant Acceptors

ARTICLE *in* THE JOURNAL OF PHYSICAL CHEMISTRY A · APRIL 2012

Impact Factor: 2.69 · DOI: 10.1021/jp3006712 · Source: PubMed

THE JOURNAL OF PHYSICAL CHEMISTRY A

Article

pubs.acs.org/JPCA

Photoinduced Electron Transfer and Nonlinear Absorption in Poly(carbazole-*alt*-2,7-fluorene)s Bearing Perylene Diimides as Pendant Acceptors

Chun Huang, Matthew M. Sartin, Matteo Cozzuol, Nisan Siegel, Stephen Barlow, Joseph W. Perry,* and Seth R. Marder*

School of Chemistry and Biochemistry and Center for Organic Photonics and Electronics, Georgia Institute of Technology, Atlanta, Georgia 30332-0400, United States

ABSTRACT: This paper reports the synthesis, photophysical behavior, and use in nanosecond optical-pulse suppression of a poly(2,7-carbazole-*alt*-2,7-fluorene) and a poly(3,6-carbazole-*alt*-2,7-fluorene) in which the carbazole *N*-positions are linked by an alkyl chain to one of the nitrogen atoms of a perylene-3,4,9,10-tetracarboxylic diimide (PDI) acceptor. It was found that the PDI pendants on the polymer side chain aggregated even in dilute solution, which extended the onset of PDI absorption into the near-infrared (NIR). Transient-absorption spectra of these polymers provide evidence for efficient electron transfer following either donor or acceptor photoexcitation to form long-lived charge-separated species, which exhibit strong absorption in the NIR. The spectral overlap between the transient species and the long-wavelength absorption edge of the aggregated PDI leads to reverse saturable absorption at 680 nm that can be used for optical-pulse suppression. Additionally, at high input energies, two-photon absorption mechanisms may also contribute to the suppression. PDI-grafted polymers exhibit enhanced optical-pulse suppression compared with blends of model materials composed of unfunctionalized poly(carbazole-*alt*-2,7-fluorene)s and PDI small molecules.

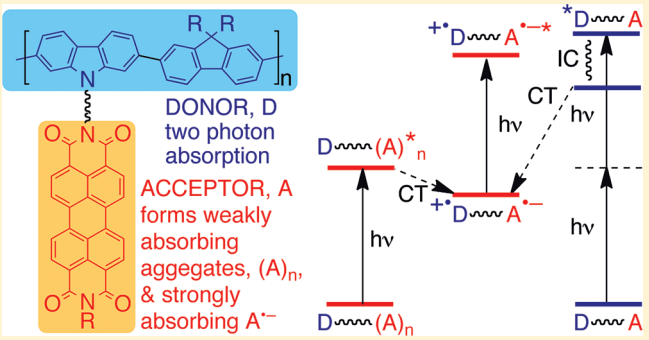

INTRODUCTION

Because of their potential use in protecting eyes and optical sensors, systems able to suppress strong optical pulses in various wavelength regions have attracted significant research interest over the past two decades.[1,2] Effective optical-pulse suppression systems require materials that maintain high transparency under low-intensity irradiation, but can respond rapidly (on the time scale of the optical pulse) to attenuate a high-intensity laser pulse. Depending on the duration and intensity of the incident pulses, different nonlinear transmission mechanisms may be useful.[1−3] Two widely used approaches are (i) to use chromophores that exhibit efficient two-photon absorption (2PA) and subsequent strong excited-state absorption (ESA) in the same spectral region,[2−5] and (ii) to use materials that exhibit reverse saturable absorption (RSA), that is, materials for which the ESA cross section (σ_e) exceeds that of the ground state (σ_g) at the wavelength of interest.[1] The effectiveness of using RSA for optical-pulse suppression is determined by the cross sections of the relevant states, with larger σ_e/σ_g generally leading to more efficient optical-pulse suppression where there is sufficiently large σ_g to allow a sizable excited-state population to be built up, and the temporal evolution of their populations during the pulse, which in turn, depends upon the relative magnitudes of the excited-state lifetime and pulse duration and on the rate of formation of the relevant excited states.[1] One approach to RSA-based optical-pulse suppression is to exploit long-lived triplet excited-state absorptions; this is feasible in cases where rapid intersystem crossing leads to high triplet populations and where the triplet cross-section is high compared to the ground-state cross-section at the wavelength of interest. For example, heavy-metal-containing phthalocyanines[6,7] or of heavy-metallopolyynes and their oligomers, especially by Wong et al.,[8−12] have proven effective for use in the 450−600 nm range.

Another approach to RSA, especially effective for use in the NIR, has recently been developed based on the formation of strongly absorbing radical ions following photoinduced intra- or intermolecular electron transfer.[13−15] Blends of polythiophene and fullerene derivatives were among the earliest reported effective optical-pulse suppression systems relying on this mechanism; the strong optical suppression observed at 700 and 760 nm was attributed to excitation of the weak long-wavelength tail of the polythiophene absorption followed by excited-state electron transfer from the polythiophene to the C_{60} derivative to give the strongly absorbing polythiophene positive polaron (radical cation).[14] Similar phenomena have been utilized in other polymer blends[15] and in molecular dyads to achieve good optical-pulse suppression at various NIR

Received: January 19, 2012
Revised: April 10, 2012
Published: April 25, 2012

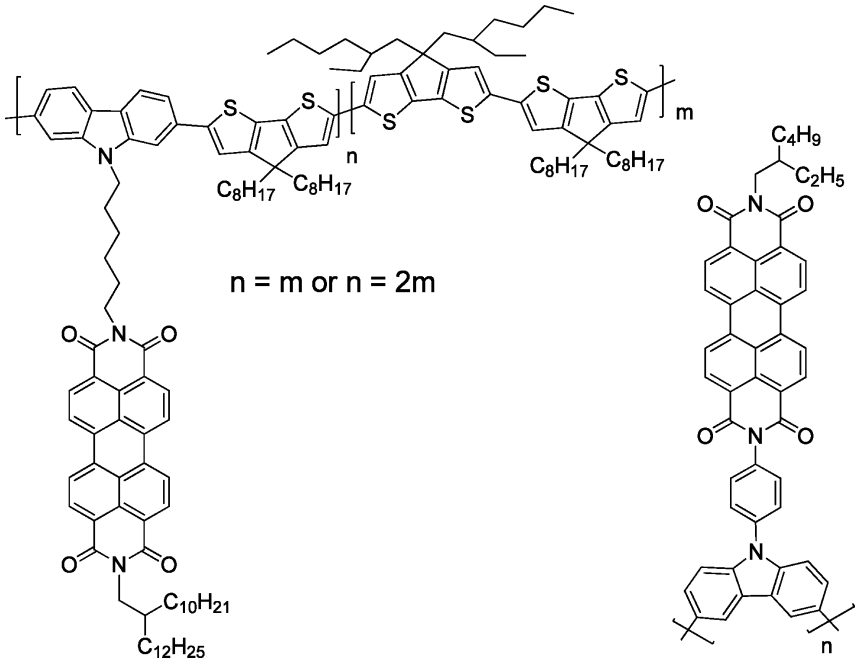

Figure 1. Two PDI-based "double-cable" polycarbazole copolymers.[19,20].

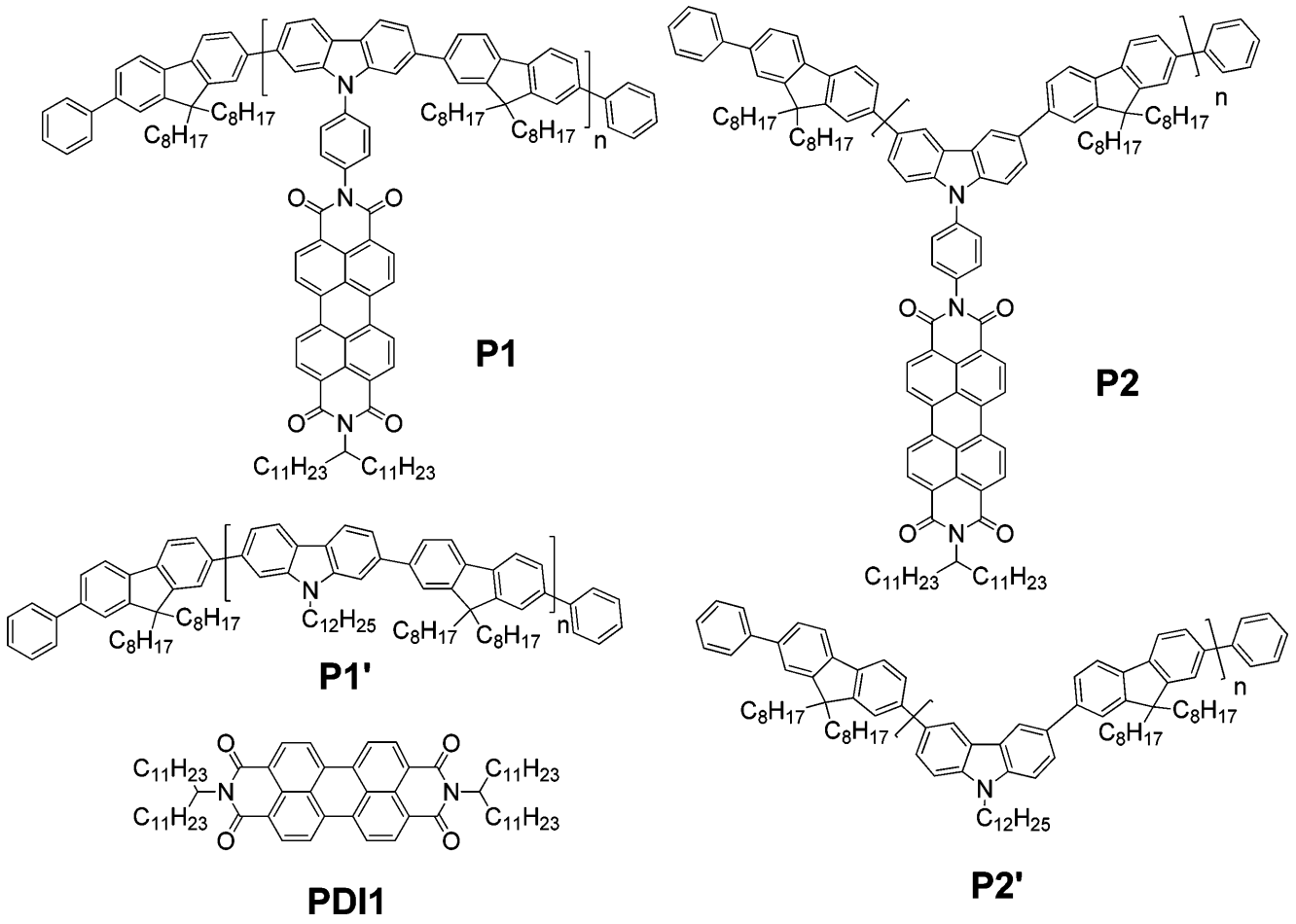

Figure 2. Chemical structures of PDI grafted polymers and the model compounds.

wavelengths.[13,16] In principle, donor−acceptor (D-A) type "double-cable" conjugated polymers,[17−21] in which electron-accepting moieties are covalently linked to an electron-donating conjugated polymer backbone can also be candidates for the application of optical-pulse suppression using the same mechanism. Rapid photoinduced charge separation and long-

dx.doi.org/10.1021/jp3006712 | J. Phys. Chem. A 2012, 116, 4305−4317

Scheme 1. Synthetic Scheme for the PDI-Grafted Polymers and Respective Model Materials

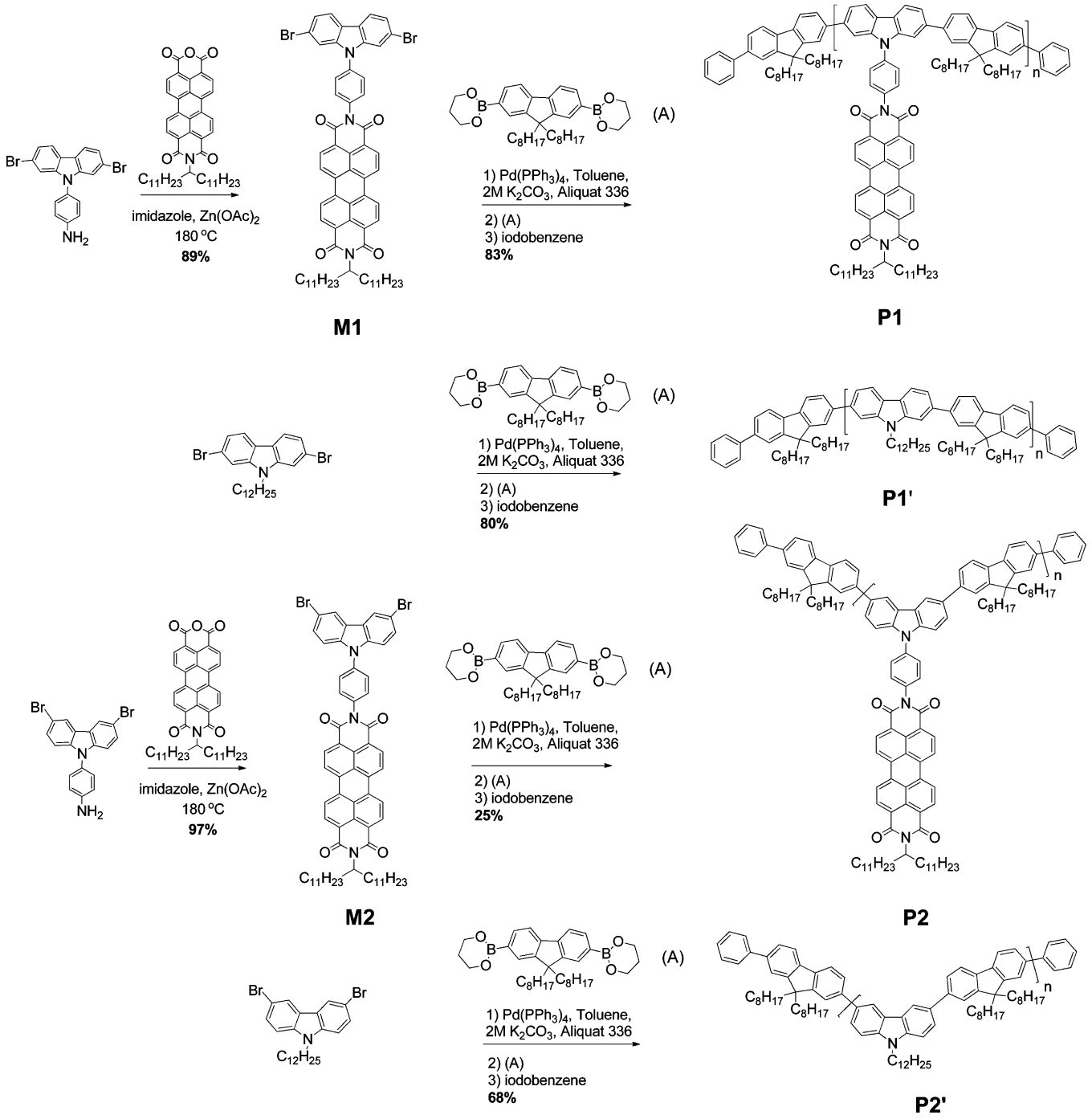

lived charge-separated states have been previously demonstrated in such materials, particularly in research on such materials for organic photovoltaics.[17−20] Moreover, because of their homogeneous molecular distribution and the relatively well-controlled distance between the donor and acceptor building blocks in these systems (at least compared to that in simple donor/acceptor material blends), "double-cable" polymers of this type could help overcome the phase-separation issues commonly encountered for physical blends, and maximize the donor−acceptor interaction in the solid state. This could potentially result in higher-quality films, because of better control of film morphology, as well as the possibility of creating a larger population of radical ions following the photoexcitation.

Perylene-3,4,9,10-tetracarboxylic acid diimides (perylene diimides, PDIs) are a group of acceptors extensively used for organic optical and electronic applications.[22−29] An interesting property of PDI-based materials is their tendency to aggregate with one another in solution or in the solid state because of their strong $\pi-\pi$ stacking interactions; these aggregates can extend the low-energy absorption edge of PDI materials beyond 600 nm.[23] In addition, the existence of long-lived charge-separated states has been demonstrated in many donor-PDI systems, and PDI radical anions exhibit several strong absorptions in the visible and NIR (ca. 600 to 1000 nm).[29−35]

dx.doi.org/10.1021/jp3006712 | J. Phys. Chem. A 2012, 116, 4305−4317

Hence, the spectral overlap between the weak low-energy tail of the PDI-aggregate ground-state absorption and the fairly strong absorption from PDI radical anions suggests the possibility of RSA-type charge-transfer optical-pulse suppression from PDI aggregates attached to suitable donor polymers.

Carbazole-containing conjugated polymers or oligomers are typically electron donors, exhibiting high hole mobility, relatively low ionization potentials, and stable radical cations (polarons). Over the past decade, carbazole-based conjugated materials have been extensively studied for organic electronic applications, resulting in high-performance devices.[36−47] Recently, efficient photoinduced electron-transfer processes have been demonstrated in PDI/polycarbazole blends or PDI-grafted D−A "double-cable" polycarbazole copolymers (Figure 1), and promising devices have been achieved using these materials as active layers in solution-processed solar cells.[19−21,48] However, to the best of our knowledge, there are no reports on using photogenerated radical-ion absorption in PDI/donor polymer blends or PDI-based D−A "double-cable" polymers for optical-pulse suppression applications.

This paper reports, the syntheses of two new poly(carbazole-*alt*-2,7-fluorene)s (PCFs) bearing PDIs on the side chains as pendant acceptors, along with the characterization and optical-pulse suppression behavior of these materials. As shown in Figure 2, the PDI moieties are covalently bound to the electron-donating poly(2,7-carbazole-*alt*-2,7-fluorene) and poly(3,6-carbazole-*alt*-2,7-fluorene) polymeric backbones in the D−A type "double-cable" polymers, **P1** and **P2**, respectively. The polymeric architecture is expected to enhance the $\pi-\pi$ stacking interaction[21] between the PDI moieties, providing sufficient ground-state from aggregated PDIs ($(PDI)_n$) for achieving optical-pulse suppression at wavelengths where the PDI radical anion absorbs strongly. In addition, 2PA absorption by the PCF backbones could also contribute to the optical suppression. In this work, a phenylene linker was chosen to covalently bind the PDI moieties on the polymer side-chain, based on previous observations of a long-lived charge-separated state in a PDI-phenylene-donor dyad.[16] PDI-grafted poly(2,7-carbazole-*alt*-2,7-fluorene), poly(3,6-carbazole-*alt*-2,7-fluorene), and model compounds for the donors (**P1′** and **P2′**) and acceptors (**PDI1**) were synthesized to investigate effects of the donor polymer architecture on the optical-pulse suppression performance of these materials.

RESULTS AND DISCUSSION

Synthesis. Many carbazole- and fluorene-containing conjugated polymers such as poly(carbazole)s,[48,49] poly(2,7-fluorene)s,[50] and poly(3,6-carbazole-*alt*-2,7-fluorene)s[51] have been synthesized for organic electronic applications, and the methods developed in these previous reports guided our synthesis of the PDI-grafted PCFs. Two new monomers containing dibromo-carbazole and PDI moieties with phenylene linkers were designed, and the desired PDI-grafted polymers were prepared following typical Suzuki polymerization procedures.[50,51] Scheme 1 outlines the synthesis of the new monomers and respective copolymers. *N*-(1-Undecyl-dodecyl)-perylene-3,4-dicarboxyanhydride-9,10-dicarboximide,[52] 4-(2,7-dibromo-9*H*-carbazol-9-yl)aniline,[53] 4-(3,6-dibromo-9*H*-carbazol-9-yl)aniline,[53] 2,7-dibromo-9-dodecyl-9*H*-carbazole,[49] and 3,6-dibromo-9-dodecyl-9*H*-carbazole[54] were prepared as described in the literature. **M1** was readily accessible through a $Zn(OAc)_2$-catalyzed condensation reaction between *N*-(1-undecyl-dodecyl)-perylene-3,4-dicarboxyanhydride-9,10-dicarboximide and 4-(2,7-dibromo-9*H*-carbazol-9-yl)aniline in molten imidazole at 180 °C. **M2** was prepared by the same method using 4-(3,6-dibromo-9*H*-carbazol-9-yl)aniline instead of 4-(2,7-dibromo-9*H*-carbazol-9-yl)aniline. The yields for these condensation reactions are in the range of 85−100%, and silica-gel column chromatography was used to purify the products. The incorporation of long "swallow-tail" chains in the PDI *N*-terminus provides the PDI-grafted monomers with excellent solubility for use in polymerizations. The chemical structures and the purity of these monomers were confirmed by ^1H and ^{13}C NMR spectroscopy, mass spectroscopy, and elemental analysis. High-molecular-weight (>15 kDa, see Table 1) alternating poly(carbazole-*alt*-2,7-fluorene)s with grafted PDI pendants (**P1** and **P2**) were then obtained through palladium-catalyzed Suzuki coupling between 2,2′-(9,9-dioctyl-9*H*-fluorene-2,7-diyl)bis(1,3,2-dioxaborinane) and **M1** or **M2** using $Pd(PPh_3)_4$ (1 mol % with respect to monomer) as the source of catalyst.[51,55] Both PDI-grafted polymers show good solubility in toluene, dichloromethane, chloroform, and tetrahydrofuran (THF), which allows optical-pulse suppression measurements to be performed in high-concentration solutions and is useful for fabricating high-quality films for solid-state measurements. The much lower yield in the synthesis of **P2** (Table 1) is associated with a large quantity of low-molecular-weight materials formed during the Suzuki polycondensations; these were removed in the subsequent purification through Soxhlet extraction with methanol and acetone. It is worth noting that it was found that $Ni(COD)_2$-catalyzed Yamamoto polycondensations of **M1** and **M2** only lead to oligomers, with only 2 or 3 repeat units, rather than high-molecular-weight polymers, despite the use of polymerization conditions similar to those reported by Müllen and coworkers to afford high-molecular-weight poly(*N*-alkyl-2,7-carbazole)s.[48] The model polymers were synthesized using similar procedures and were found to have higher molecular weights and larger polydispersities (see Table 1). These model polymers, especially **P2′**, also show high solubility in common organic solvents such as toluene, chlorobenzene, THF, and chloroform (>10 mg/mL) at ambient temperature; however, **P1′** exhibits limited solubility in dichloromethane (<1 mg/mL).

Table 1. Polymerization Results and Thermal Properties of the Polymers

polymer	yield	M_n (kDa)	M_w/M_n	T_d (°C)	T_g (°C)	T_m (°C)
P1	83%	15.4	3.68	388	277	N.A.
P2	26%	18.1	1.91	390	210	N.A.
P1′	80%	61.1	4.00	409	160	ca. 280
P2′	68%	24.5	3.55	412	95	N.A.

Thermal Properties. As shown in Figure 3 and Table 1, all polymers exhibited good thermal stability, with the decomposition temperatures (T_d), defined as that at which 5% weight loss is observed using thermogravimetric analysis, exceding 385 °C under nitrogen, the PDI-containing polymers showing values of T_d about 20 °C lower than those for the model polymers, presumably because of either degradation of the PDI aromatic core or its "swallow-tail" substituent. The thermal behavior of these polymers was also investigated by differential scanning calorimetry (DSC) from −25 to 300 °C under nitrogen atmosphere. Glass-transition temperatures (T_g) were in excess of 200 °C for the PDI-functionalized polymers, considerably higher than those for **P1′** and **P2′** (Table 1),

dx.doi.org/10.1021/jp3006712 | J. Phys. Chem. A 2012, 116, 4305−4317

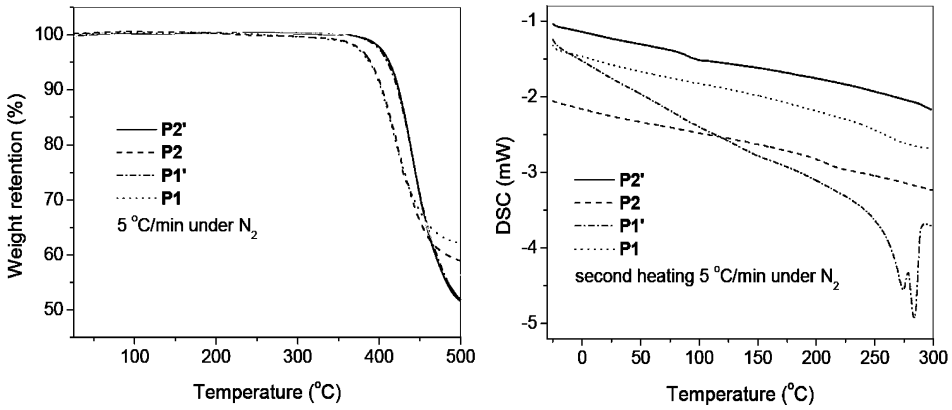

Figure 3. TGA traces (left) and DSC traces (right) of the polymers under nitrogen.

perhaps because of strong $\pi-\pi$ interactions between the side-chain PDI groups in the solid state. **P1′** melts at about 280 °C under nitrogen, while no obvious melting transition was observed for the other three polymers. The good thermal stability and high glass-transition temperatures are attractive attributes from the point of view of using these polymers as active materials for organic optical and electronic applications.

Linear Absorption and Emission Properties. As shown in Figure 4, the solution UV−vis absorption spectra of **P1** and **P2** in toluene (ca. 10^{-5} M, based on the polymer repeat unit) are essentially superpositions of the characteristic absorption bands of the polymer models and of aggregated PDIs.[23,56] The absorption maxima of **P1′** and **P2′** are slightly bathochromically shifted relative to the corresponding bands from the analogous PDI-grafted polymers; this may be tentatively ascribed to a shorter conjugated polymer backbone because of the relatively lower molecular weight of PDI-grafted polymers and/or the PDI pendants leading to less intermolecular packing between the polymer backbones. In the polymers with PDI pendants, the ratio of the absorbance of the (0,0) vibronic sub-band of the PDI absorption to that of the (0,1) sub-band was found to be significantly smaller than the value of 1.66 typical for nonaggregated PDIs (1.23 for **P2** and 1.13 for **P1**), suggesting substantial aggregation of the PDI side-chains, even in dilute toluene solution (ca. 10^{-5} M).[21,23,56] In more concentrated toluene solution (ca. 10^{-3} M), significant absorption can be detected in the 600−800 nm range for **P1** and **P2**, as illustrated in Figure 5. The molar absorption coefficients for both **P1** and **P2** are more than 200 M^{-1} cm^{-1} at 700 nm and larger than 500 M^{-1} cm^{-1} at 650 nm, respectively, in toluene, higher than the corresponding values of **PDI1** in the same spectral region at similar concentration (ε_{700} < 10 M^{-1} cm^{-1}, concentration-independent, even up to 10 mM).[16] This significant enhanced NIR absorption might originate from $(PDI)_n$ absorption, while the weak absorption band seen for concentrated solutions of **P2** at about 920 nm might be attributable to absorption from an

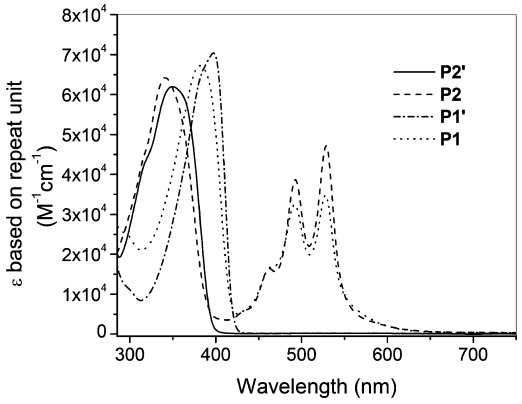

Figure 4. Linear absorption spectra of the polymers in dilute toluene solution.

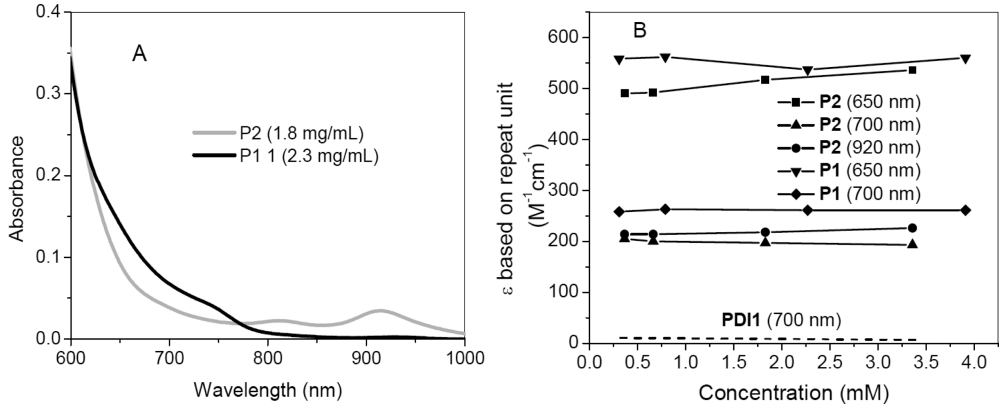

Figure 5. (A) Absorption spectra of the PDI-grafted polymers in highly concentrated toluene solutions. The band peaked at 920 nm for **P2** is tentatively attributed to ground-state intermolecular or intramolecular charge-transfer complexes; (B) molar absorptivities of the PDI-grafted polymers in highly concentrated toluene solution at different wavelengths.

dx.doi.org/10.1021/jp3006712 | J. Phys. Chem. A 2012, 116, 4305−4317

intra- or intermolecular ground-state charge-transfer complex between the PCF backbone and PDI pendants, similar to that seen in some previously reported donor-PDI systems.[16,57] The molar absorptivities in the NIR range for **P1** and **P2** are not significantly dependent on the PDI concentration in toluene solution (at least in the concentration range of 0.1 to 3 mM), perhaps indicating saturated aggregation in the investigated concentration range for the grafted PDI moieties on the polymer side-chains.

The emission spectra of the PDI-grafted polymers and the model compounds in toluene are shown in Figure 6. The

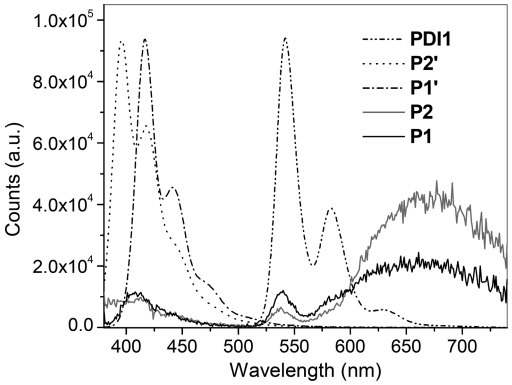

Figure 6. Emission spectra of the PDI grafted polymers and respective model compounds in toluene. **P1** and **P2**, as well as the respective model polymers, were excited at 375 nm. The **PDI1** emission spectrum was collected using excitation at 490 nm.

emission spectra of the polymer polymers show characteristic features of both the respective donor polymer, nonaggregated PDI molecules (peaked at ca. 535 nm), and PDI aggregates (peaked at ca. 650 nm).[58] The observation of PDI-aggregate-type emission is consistent with the PDI-aggregate-type UV–vis absorption spectra (see above).[21,58] The PDI-based emission observed upon 375 nm excitation of the PDI-grafted polymers could result either from energy transfer from the excited donor polymer backbone to the PDI units or from direct excitation of the weak UV absorption of the PDI units (<10% of the total absorption at 375 nm). The excitation spectra of **P1** and **P2** obtained while monitoring the emission at 620 nm are shown in Figure 7. These spectra show the characteristic absorption bands of the donor polymer backbone, a vibrationally structured PDI absorption, and PDI aggregate

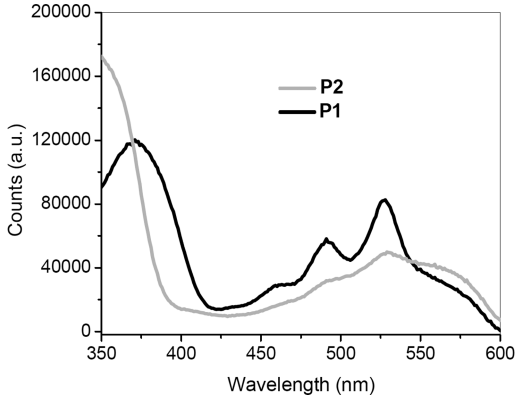

Figure 7. Excitation spectra of **P1** and **P2** in toluene acquired using a fixed emission wavelength of 620 nm.

absorption. The relatively weak contribution of the structured PDI feature to the excitation spectra suggest that the observation of emission from both donor and acceptor species following excitation at 375 nm is primarily a result of energy transfer from the photoexcited donor polymer backbone. The fluorescence quantum yields observed for the PDI-grafted polymers (0.5% and 0.7% for **P1** and **P2**, respectively, when excited at 375 nm) are much lower than that for **PDI1** (83% in toluene, excited at 490 nm) and aggregated PDIs (generally between 20% and 50%),[59,60] or the polymer models (65% and 56% for **P1′** and **P2′** in toluene, respectively). The reduced emission from the PDI-grafted polymers relative to the respective model compounds indicates quenching of the excited states, consistent with photoinduced electron transfer.

Radical-Ion Absorption Spectra. Chemical oxidation and reduction of model donors and acceptor, respectively, was carried out to establish the wavelengths at which charge-transfer optical pulse suppression might be feasible and to aid with the interpretation of transient absorption spectra (see below). Positive polarons were generated in the model polymers in dichloromethane by addition of a large excess of **P1′** or **P2′** to a dilute solution of tris(4-bromophenyl)aminium hexachloroantimonate.[61] The radical anion of the **PDI1** was prepared in THF by using cobaltocene under nitrogen.[62] The resulting radical-ion absorption spectra are shown in Figure 8. The

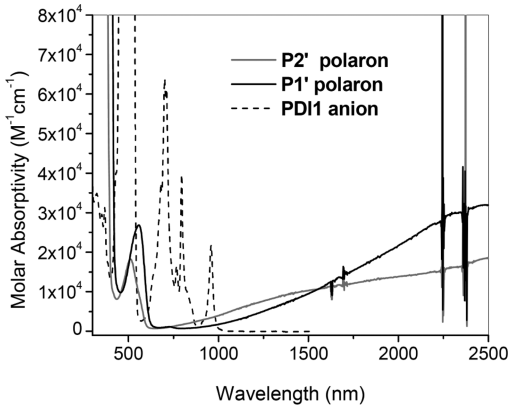

Figure 8. Polaron absorption of the **P1′** and **P2′**, in dichloromethane and the **PDI1** radical-anion absorption in THF.

absorption maximum of the polaron from **P1′** in the UV–vis range is around 560 nm. This shows a bathochromic shift of about 50 nm compared with the polaron generated from **P2′**, presumably because of the cross-conjugation in the polymer backbone of **P2′**. The polarons of **P1′** and **P2′** also exhibit strong, but broad, absorption bands in the NIR region. The absorption spectrum of the **PDI1** radical anion (Figure 6) is similar to those of other PDI radical anions with similar chemical structures shown in literature, exhibiting peaks at 698, 798, and 958 nm.[22,29,63]

Redox Properties. The electrochemical behavior of **P1**, **P2** and respective model polymers was investigated by cyclic voltammetry (CV). The measurement was performed under nitrogen, in a solution of tetrabutylammonium hexafluorophosphate (0.10 M) in anhydrous acetonitrile at a scan rate of 50 mV/s using the polymer films drop-cast onto a platinum working electrode from 2 mg/mL polymer solutions in chloroform. Separate oxidative and reductive scans were carried out for the film samples. The results are summarized in Table 2,

dx.doi.org/10.1021/jp3006712 | J. Phys. Chem. A 2012, 116, 4305–4317

Table 2. Summary of the Optical and Electrochemical Properties of the Polymers

polymer	λ_{max}^{abs} (nm)	λ_{max}^{em} (nm)	η^{em} (%)	E_g^{opt} (eV)[a]	E_{ox}^{onset} (V)[b]	E_{red}^{onset} (V)[b]	ΔG_{CS}^{D*} (eV)[c]	ΔG_{CS}^{A*} (eV)[c]
P1	381, 491, 528	408, 539, 661[e]	ca. 0.5[f]	2.1	+0.44	−1.04	−1.4	−0.7
P2	340, 491, 527	538, 667[e]	ca. 0.7[f]	2.1	+0.55	−1.06	−1.5	−0.5
P1′	386	417, 441	65[f]	2.9	+0.40	N.A.		
P2′	349	396, 418	56[f]	3.1	+0.54	N.A.		
PDI1	459, 490, 527	541, 582, 630	83[g]	2.2	N.A.	−1.01[d]		

[a] E_g (optical gap) was estimated from the absorption on-set of UV absorption of respective materials at low concentration (ca. 10^{-5} M). [b] Versus ferrocenium/ferrocene. [c] Free-energy changes for excited-state donor-to-PDI electron transfer from donor or acceptor-based excited states (D* and A* respectively), estimated according to $\Delta G_{CS} = eE_{ox}^{onset} - eE_{red}^{onset} - E_g(\text{optical})$, where the value of E_g(optical) used is that of the appropriate model polymer and of the model PDI for ΔG_{CS}^{D*} and ΔG_{CS}^{A*} respectively. [d] $E_{1/2}^{0/-}$ obtained from solution measurement in dichloromethane. [e] λ_{max}^{em} values for the low-energy emissions are approximate and were estimated after smoothing the emission spectra shown in Figure 6. [f] Excitation at 375 nm. [g] Excitation at 490 nm.

and the cyclic voltammograms of the polymers and **PDI1** are shown in Figure 9. The reduction potentials for **P1** and **P2** are

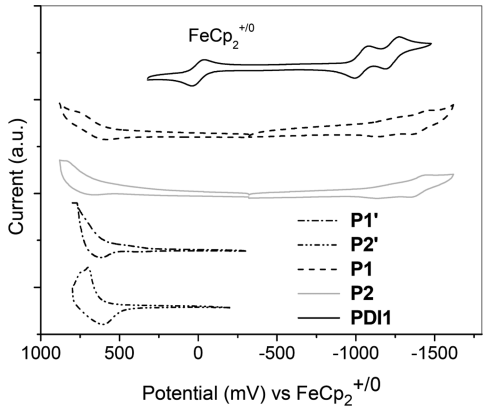

Figure 9. Cyclic voltammograms of polymer films drop-cast from ∼2 mg/mL $CHCl_3$ solution onto a Pt working electrode in acetonitrile with 0.1 M tetra-*n*-butylammonium hexafluorophosphate, except for **PDI1**, for which the CV was performed in dichloromethane solution. Potential was scanned at a rate of 50 mV/s.

similar to that of the **PDI1** (for which a CV measurement was performed using a dichloromethane solution). The similarity of the potentials for the PDI-grafted polymers to those for the model compounds suggests weak ground-state electronic-coupling between the PDI pendants and donor polymer backbones, consistent with the UV−vis absorption spectra (see above). The free-energy changes for electron transfer from either a donor-based excited-state to the pendant PDI or from the donor polymer backbone to the PDI excited-state, ΔG_{CS}^{D*} and ΔG_{CS}^{A*}, respectively, estimated using the electrochemical potentials and the absorption onsets[64] from the appropriate model compounds (see Table 2) are highly exergonic, even when Coulombic stabilization of the resultant ion pair is neglected, confirming the energetic feasibility of obtaining the excited-state electron-transfer in these systems.

Transient Absorption. Femtosecond (fs) laser pulse transient-absorption spectra of the model materials are shown in Figure 10. **PDI1** shows excited-state absorption peaked at about 680 nm, with a lifetime that exceeds the temporal range of our experimental setup, and **P1′** and **P2′** exhibit broad excited-state absorption between 400 to 800 nm with lifetimes shorter than 1.5 ns.

Transient-absorption spectra of the PDI grafted PCFs, **P1** and **P2**, in toluene, generated by pumping the PDI moiety at 530 nm or primarily the donor polymer backbone at 350 nm

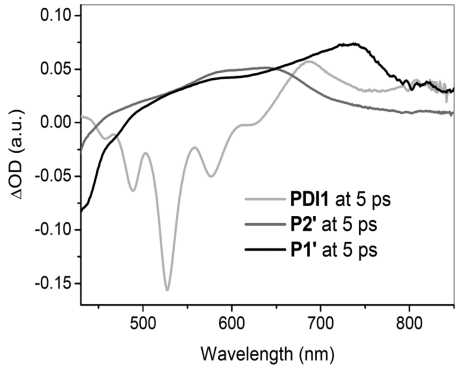

Figure 10. Femtosecond laser pulse transient absorption at 5 ps after excitation of **PDI1** (excited at 425 nm), **P2′** (excited at 350 nm), and **P1′** model (excited at 350 nm) in toluene (absorbances at the excitation wavelengths were ca. 0.3).

with femtosecond laser pulses, are shown in Figure 11. Shortly after the photoexcitation of the PDI moieties of **P1**, a feature peaked at 680 nm and attributable to PDI excited-state absorption (Figure 10) is observed. This is followed by the rapid (<5 ps) growth of absorption bands with peaks at about 580 and about 710 nm. Comparison with chemically oxidized and reduced species above suggests these features can be assigned to the **P1′** postive polaron and to the PDI radical anion, respectively, that is, there is efficient electron transfer from the polymer backbone to the PDI excited state to form an ion pair. Excitation of **P1** at 350 nm, that is primarily exciting the polymer backbone, with femtosecond laser pulses, leads initially (0.3 ps) to spectra essentially identical to those seen for model polymer **P1′** (Figure 10,11), followed by rapid growth of the 580 and 700 nm absorptions (<1.5 ps) consistent with formation of the ion pair. The transient absorption-spectra obtained from **P2** by pumping of either donor or acceptor were similar to those of **P1** although no donor polymer radical-cation absorption was observed in the transient absorption spectra of **P2**, presumably because of the spectral overlap between the polaron absorption, peaked at about 500 nm, and the PDI ground-state bleach. The spectrum of **P2** obtained 1.5 ps after excitation at 350 nm shows a small dip at 575 nm absent from the 0.3 ps spectrum that may correspond to the stimulated emission peak observed from direct excitation of the PDI moiety. Its late appearance suggests energy transfer may play a role in the overall mechanism of charge-separation from the polymer-based excitation, consistent with fluorescence data. The lifetimes of the charge-separated states for both PDI grafted polymers are longer than 3 ns, which is the maximum time delay achievable using our instrumentation. Excitation of

dx.doi.org/10.1021/jp3006712 | J. Phys. Chem. A 2012, 116, 4305−4317

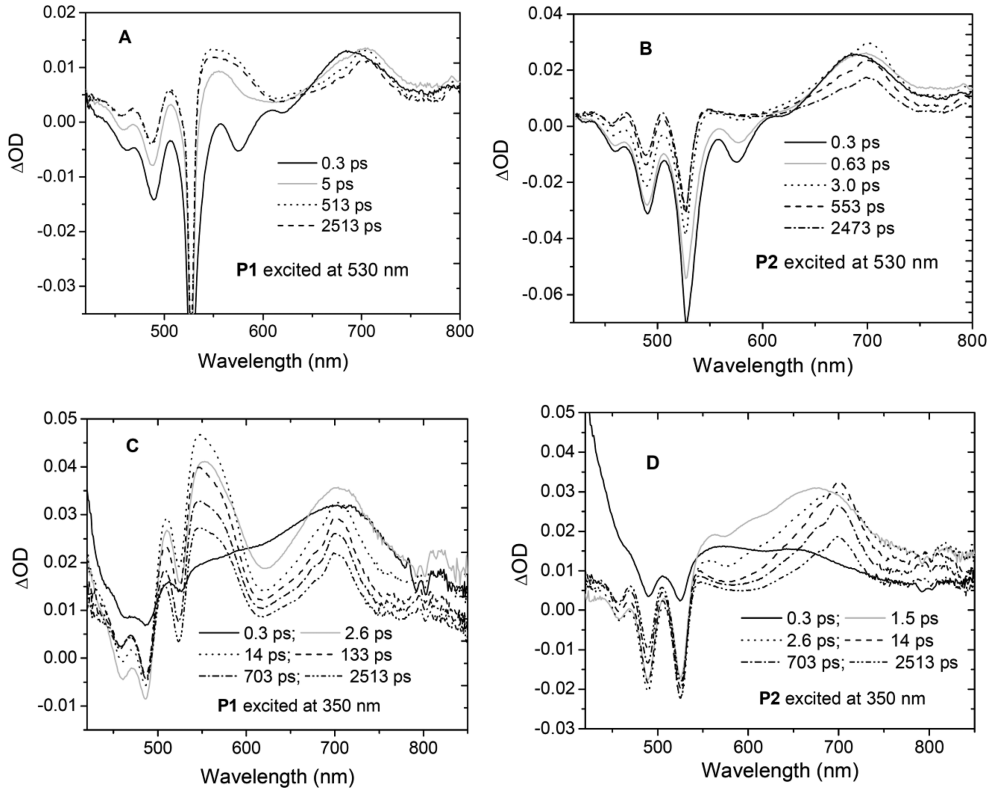

Figure 11. Femtosecond transient-absorption spectra of **P1** (A) and **P2** (B) in toluene excited at 530 nm. Transient-absorption spectra of **P1** (C) and **P2** (D) in toluene following excitation at 350 nm. All samples were prepared to be ca. 30 μM in toluene in a 2 mm cuvette to yield an absorbance of ca. 0.3 at the excitation wavelength.

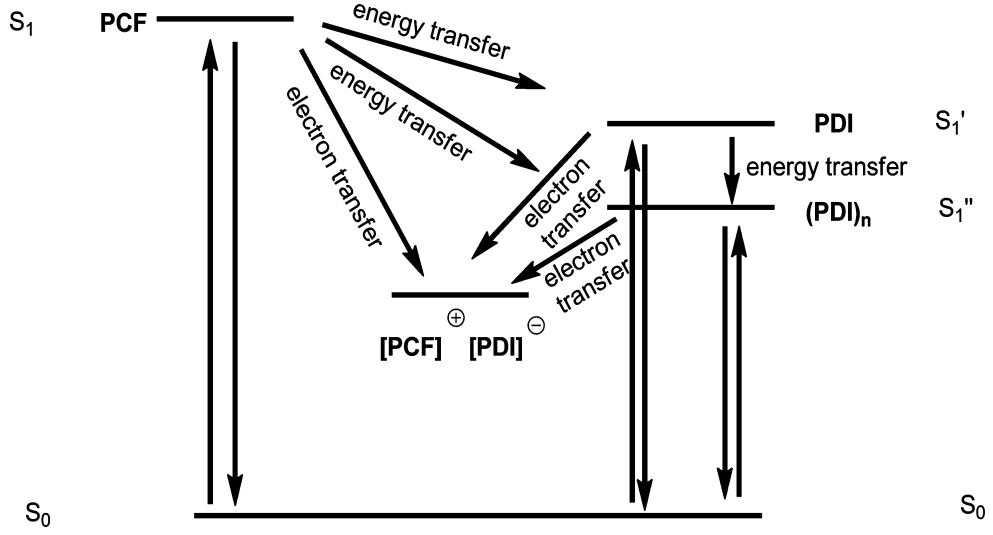

Figure 12. Proposed energy level diagram showing the lowest excited singlet states of PCF and nonaggregated PDI, of the aggregates $(PDI)_n$, and that of the charge-transfer state. The arrows show the processes that might occur upon photoexcitation of PCF or PDI.

PDI aggregates at 680 nm in highly concentrated polymer solution (ca. 4 mg/mL in toluene) also results in long-lived charge-separated states and a fairly strong transient-absorption band between 600−800 nm, which demonstrates the possibility of optical-pulse suppression at these wavelengths.

The results of the transient absorption measurements together with the emission study in solution can be summarized in a Jabłoński diagram (Figure 12). After photoexcitation of the donor polymer backbone (PCF), the excited state is largely quenched by energy and electron transfer from the PCF excited-states to PDI or $(PDI)_n$, leading to low fluorescence quantum yields. The newly generated PDI- or $(PDI)_n$-based excitons are quenched predominantly via electron-transfer by accepting an electron from PCF. If PDI or $(PDI)_n$ are photoexcited directly, these PDI-based excited-states could be quenched in the same way, that is, by electron-transfer from PCF, forming the PDI radical anion and donor polymer polaron (or by other radiative and nonradiative decay mechanisms).

dx.doi.org/10.1021/jp3006712 | J. Phys. Chem. A 2012, 116, 4305−4317

Nonlinear Absorption and Optical Pulse Suppression. The optical-pulse suppression behavior of **P1** and **P2** upon photoexcitation with a 680 nm laser pulse (6 ns pulse width) is shown in Figure 13, along with those of the blend of **P1′**/**PDI1**

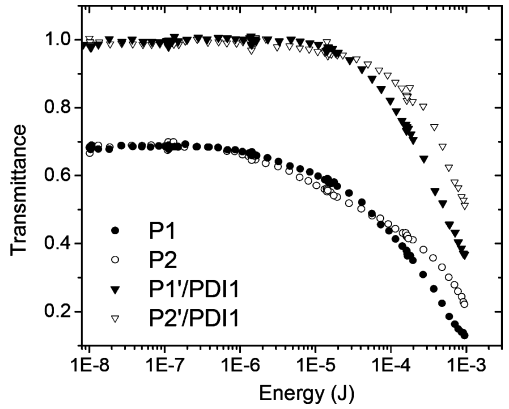

Figure 13. Optical pulse suppression of 680 nm, 6 ns pulses focused in an f/5 geometry into the center of a 2 mm, N_2-purged cell containing **P1** and **P2** (2.5 and 3.1 mM/subunit in toluene respectively) and the respective polymer model compounds mixed with **PDI1**, each at ca. 3.5 mM, in toluene.

or **P2′**/**PDI1** (~3.5 mM: 3.5 mM in toluene) solution in a 2 mm cuvette. **P1** and **P2** samples were prepared at high concentration (2.5 mM for **P1** and 3.1 mM for **P2** in toluene, based on the repeat unit concentration) to ensure about 70% linear transmittance of the samples. Both PDI-grafted polymers showed noticeable optical-pulse suppression starting at lower input energy as compared with the blend samples, even when the model blend systems had higher material concentration. The optical-pulse suppression phenomena of the model materials blends at high energy is presumably attributable to 2PA, followed by excited-state absorption or possibly absorption by some intermolecularly charge-separated species. The 2PA spectra of the two model polymers in toluene acquired using the two-photon-excited fluorescence method[65,66] (Figure 14) show 2PA cross sections (based on polymer repeating units) at 680 nm of 350 and 50 GM for **P1′** and **P2′**, respectively, while both polymers show excited-state absorption at the same wavelength (Figure 10). The much larger 2PA cross section for **P1′** is presumably at least partly responsible for its stronger optical-pulse suppression response

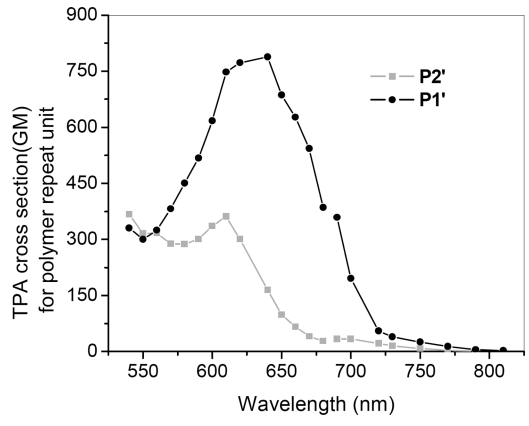

Figure 14. 2PA spectra of **P1′** and **P2′** in 100 μM solution in toluene.

at 680 nm, although differences in excited-state cross-section are also likely to be important. A measure of the strength of the nonlinear attenuation of the laser pulses is the optical suppression (defined here as $S = T_o/T_F$, where T_o is the linear transmittance, and T_F is the transmittance just below the damage fluence of the cell). The S values of the **P1** and **P2** solution here are 5.3 and 3.3, and using 680 nm excitation, respectively (Table 3). These values of S compare favorably with those obtained from porphyrin-viologen dyads[13] (S = 2.4 at 600 nm) for which a one-photon-induced charge separation mechanism provided the nonlinear absorption, as well as with those for triphenylamine-PDI based materials[67] that combined 2PA with ESA (S = 3.5 at 660 nm using picosecond pulse excitation), but are lower than those for our previous reported PDI-based molecular dyads[16] (S = 17 at 700 nm) that operated primarily via 2PA-induced ion-pair absorption. The enhanced optical-pulse suppression behavior of the PDI-grafted polymers at high pulse energy relative to that seen in the model blends may be attributed to one-photon-induced charge separation through excitation of the PDI aggregates and/or ground-state charge-transfer complexes (S values of **P1′**/**PDI1** or **P2′**/**PDI1** are 2.7 and 2.0, at 680 nm respectively). Additionally, the threshold energies, defined as the energy at which the transmittance is $T_o/2$, show stronger optical-pulse suppression at lower energies for the PDI-functionalized polymers than for the corresponding model material blends. At high pulse energy, two-photon excitations of the donor polymer backbones are also likely to contribute to the pulse suppression in **P1** and **P2**. At lower energies, slightly stronger optical-pulse suppression can be observed for **P2** than for **P1** at 680 nm. However, at higher pulse energies (ca. $E > 10^{-4}$ J), a steeper slope can be observed for **P1** over **P2**, indicating stronger optical-pulse suppression at these pulse energy for **P1** against 680 nm laser pulses. This could be attributed to the much larger 2PA cross-section at 680 nm of the 2,7-carbazole-based backbone than its 3,6-carbazole analogue, which leads to higher excited-state and PDI-radical-ion populations that could contribute to the nonlinear absorption for **P1** at energies where two-photon excitation is more significant.

■ CONCLUSION

We have prepared two new polymers with conjugated poly(carbazole-*alt*-2,7-fluorene)s as the electron-donating polymer backbones and PDI moieties incorporated into the side chains as pendant electron acceptors. Efficient photoinduced charge transfer in these copolymers in generating the respective ion-pairs was confirmed by the transient-absorption spectra. Long-lived charge-separated states with strong absorption between 600−800 nm were observed following photoexcitation of either the PDI or the donor polymer absorptions. Moreover, the PDI-grafted copolymers exhibited stronger enhancement of the nonlinear optical absorption compared with blends of the model compounds at 680 nm. This is attributed to the combination of one-photon absorption from the aggregated PDI and possible 2PA from the polymer backbones. The poly(2,7-carbazole-*alt*-2,7-fluorene) derivative, **P1**, shows stronger optical-pulse suppression at 680 nm than its poly(3,6-carbazole-*alt*-2,7-fluorene) derivative **P2**, especially of higher energy laser pulses, probably because of the larger 2PA cross section at 680 nm for **P1**.

dx.doi.org/10.1021/jp3006712 | J. Phys. Chem. A 2012, 116, 4305−4317

Table 3. Summary of the Optical Pulse Suppression Performance of the PDI Grafted Polymers and Respective Material-Blends

	P1 (2.5 mM)	P2 (3.1 mM)	P1′/PDI1 (3.5 mM)/(3.5 mM)	P2′/PDI1 (3.5 mM)/(3.5 mM)
linear transmittance	0.68	0.68	0.96	0.97
threshold energy (μJ)	200	440	520	910
T_o/T_F	5.3	3.3	2.7	2.0

EXPERIMENTAL SECTION

General Procedures. Most organic and inorganic chemicals were obtained from Aldrich and Alfa Aesar. Palladium-based catalysts were purchased from Strem Chemicals and used without further purification. ^{1}H and ^{13}C{^{1}H} NMR spectra were collected on Bruker 400 or 500 MHz spectrometers using tetramethylsilane (TMS; δ = 0 ppm) as an internal standard. Mass spectra were measured on an Applied Biosystems 4700 Proteomics Analyzer using MALDI mode. Elemental analyses were carried out by Atlantic Microlabs using a LECO 932 CHNS elemental analyzer. Solution UV−vis, absorption spectra were recorded on a UV3101PC (Shimadzu, Kyoto, Japan) absorbance spectrophotometer. The solution emission spectra and excitation spectra of toluene solutions were recorded using a Shimadzu FP-5301PC spectrofluorometer. For electrochemical measurements, the polymer films were drop-cast onto a platinum disk working electrode from a 2 mg/mL polymer solution in chloroform. A platinum wire served as the auxiliary electrode, and an Ag wire anodized with AgCl served as a pseudoreference electrode. The experiments were performed on deoxygenated 0.1 M solutions of tetra-*n*-butylammonium hexafluorophosphate in anhydrous acetonitrile at a scan rate of 50 mV s^{-1}, using a computer-controlled BAS 100B electrochemical analyzer. Potentials were referenced to the ferrocenium/ferrocene ($FeCp_2^{+/0}$) couple by using ferrocene as an external standard. Thermogravimetric analysis measurements were performed on an NETZSCH STA 449C analyzer under 40 mL/min N_2 flow with a heating rate of 5 °C/min. Differential scanning calorimetry measurements were performed on a TA Instruments DSC Q200 analyzer under 50 mL/min N_2 flow with heating rate of 5 °C/min.

Generation of Radical Ions. The radical anion of the **PDI1** was generated in anhydrous THF solution by reduction with cobaltocene in a nitrogen atmosphere glovebox. The radical cation of **P1′** or **P2′** was generated in anhydrous dichloromethane after oxidation with tris(*p*-bromophenyl)-aminium hexachloroantimonate. The spectra of the radical ions were recorded with a Varian Cary 5E UV−vis−NIR spectrophotometer using 1 cm path length cells under nitrogen.

Two-Photon Absorption Spectroscopy. 2PA spectra were obtained using the reference-based two-photon-excited fluorescence (2PEF) method.[66,68] The excitation source was an optical parametric oscillator (Quanta-Ray MOPO 730) pumped by 6 ns pulses from the third harmonic of a Q-switched Nd:YAG laser (Quanta-Ray PRO250). The 2PEF method determines the 2PA spectra of unknowns by measuring the fluorescence emitted by the unknowns under two-photon excitation conditions and comparing it to the fluorescence emitted by a known reference compound under the same conditions. The 2PEF measurements of the model compounds were carried out in toluene (Sigma-Aldrich spectroscopic grade) solution at chromophore concentrations of 80−110 μM. The data shown here comprise several collections of over 200 pulses at each wavelength. 1,4-bis(2-methylstyryl)-benzene[65,69] (Sigma-Aldrich, 99%) in cyclohexane (Sigma-Aldrich, spectroscopic grade) and fluorescein[66] (Acros, laser grade) in aqueous NaOH solution (pH 11) were used as references for the 630−680 nm and 690−1040 nm ranges, respectively. The 2PA cross-section values of 1,4-bis(2-methylstyryl)benzene reported by Kennedy and Lytle[69] were reduced in scale by a factor of 10, as described by Fisher et al.[65] The uncertainties in the measured cross sections are approximately ±15%.

Femtosecond Transient-Absorption Measurements. The excitation source for femtosecond transient-absorption measurements was generated by an optical parametric amplifier (TOPAS, Newport) pumped by a Ti:Sapphire regenerative amplifier (Spitfire, Newport), operating at 1 kHz repetition rate. The 800 nm Spitfire output could be varied by the TOPAS over 465−2900 nm. Approximately 5% of the 800 nm Spitfire output was used to generate the white light continuum probe beam (420−950 nm) in a sapphire plate. Transient data were collected using a commercially available Helios spectrometer (Ultrafast Systems, Sarasota, FL). The time resolution for this system is pulse-width limited at 200 fs, and the maximum time delay was 3.2 ns. At each temporal delay, the signal was averaged for 1 s. The pump beam was chopped at 500 Hz to alternate between signal and reference data. A correction factor for the chirp of the white light was generated using the ultrafast response of CCl_4. All samples were prepared in 2 mm cuvettes and deaerated with N_2. The pump wavelengths were 530 nm for the PDI-grafted polymers. The pump energy for all samples was about 3.3 μJ/pulse.

Nanosecond Optical-Pulse Suppression Measurements. The excitation source for optical-pulse suppression measurements was the same as for the ns TA measurements. A mechanical shutter reduced the pulse repetition rate to 1 Hz to minimize damage to the sample. The samples were prepared as deaerated solutions in 2 mm cuvettes, with transmittance of about 0.7 at the excitation wavelength of 680 nm. The laser was focused into the center of the cuvette using an f/5 geometry, and the transmitted light was detected by a New Focus photoreceiver (San Jose, California), sampled using a Stanford Research Systems boxcar average (Sunnyvale, CA), and recorded on a 300 MHz Tektronix oscilloscope (Richardson, Texas). A beam splitter placed before the sample redirected part of each pulse to a reference photoreceiver to determine fluctuations in the input energy of each pulse. The focus of the laser was positioned in the center of the 2 mm cell by translating the cell through the focus along the axis of the beam, while exciting the sample with 1 μJ pulses (z-scan). Reverse saturable absorption reduced the transmitted signal while the sample was passing through the focus, so the position where the focus was in the middle of the cuvette could be determined from the middle of the region of reduced transmittance.

M1. *N*-(1-Undecyl-dodecyl)-perylene-3,4-dicarboxyanhydride-9,10-dicarboximide[52] (0.356 g, 0.50 mmol), 4-(2,7-dibromo-9*H*-carbazol-9-yl)aniline[53] (0.413 g, 0.99 mmol), anhydrous zinc acetate (80 mg, 0.44 mmol), and imidazole (3.0 g) were heated under N_2 at 180 °C overnight. The reaction mixture was then allowed to cool to about 130 °C before being poured into a 4 N aqueous HCl solution (200

dx.doi.org/10.1021/jp3006712 | J. Phys. Chem. A 2012, 116, 4305−4317

mL). The resultant red precipitate was filtered and washed sequentially with 2 N aqueous HCl (3 × 10 mL), water (3 × 10 mL), and MeOH (3 × 10 mL). The solid was then dissolved in $CHCl_3$ (5 mL), and a minimum amount of silica gel was added to adsorb the material. After the solvent was removed under reduced pressure, the dried silica gel was added to the top of a hexane-packed silica gel column, and the column was eluted with $CHCl_3$ to give **M1** as a red solid (0.53 g, 89%). ^{1}H NMR (500 MHz, $CDCl_3$): δ 8.78 (d, J = 8.0 Hz, 2H), 8.72−8.66 (m, 6H), 7.95 (d, J = 8.5 Hz, 2H), 7.75 (d, J = 8.5 Hz, 2H), 7.68 (d, J = 1.0 Hz, 2H), 7.65 (d, J = 8.5 Hz, 2H), 7.42 (dd, J = 8.5, 1.0 Hz, 2H), 5.18 (m, 1H), 2.26 (m, 2H), 1.86 (m, 2H), 1.29−1.21 (m, 36H), 0.83 (t, J = 6.5 Hz, 6H). ^{13}C{^{1}H} NMR (125 MHz, $CDCl_3$): δ 165.0, 164.1, 163.9, 141.8, 137.2, 135.8, 134.9, 134.6, 134.5, 132.4, 132.3, 131.6, 131.2, 130.2, 129.9, 128.9, 128.0, 127.0, 126.7, 124.6, 124.4, 123.9, 123.8, 123.6, 123.5, 123.3, 122.3, 122.0, 121.8, 120.6, 116.4, 113.6, 113.5, 55.3, 32.8, 32.3, 30.2, 30.1 (3 peaks), 30.0, 29.8, 27.5, 23.2, 14.7 (The observation of three carbonyl carbon resonances is consistent with previous work on perylene bis(dicarboxyimide)s using similar, swallow-tailed *N*-substituents, in which this has been attributed to restricted rotation about the N−C_{alkyl} bonds.[71] Two aromatic carbon peaks and one alkyl carbon were not observed, presumably because of overlap). HRMS (MALDI) calcd for $C_{65}H_{65}Br_2N_3O_4$ (M^+): 1109.33, found: 1109.35. Anal. Calcd for $C_{65}H_{65}Br_2N_3O_4$: C, 70.20; H, 5.89; N, 3.78. Found: C, 69.99; H, 5.92; N, 3.81. for $C_{65}H_{65}Br_2N_3O_4$: C, 70.20; H, 5.89; N, 3.78.

M2. *N*-(1-Undecyl-dodecyl)-perylene-3,4-dicarboxyanhydride-9,10-dicarboximide[52] (0.356 g, 0.50 mmol), 4-(3,6-dibromo-9*H*-carbazol-9-yl)aniline[53] (0.450 g, 1.08 mmol), anhydrous zinc acetate (80 mg, 0.44 mmol), and imidazole (3.5 g) were heated under N_2 at 180 °C overnight. The reaction mixture was then allowed to cool to about 130 °C and poured into 4 N aqueous HCl (160 mL). The resultant red precipitate was filtered and washed sequentially with 2 N aqueous HCl (3 × 10 mL), water (3 × 10 mL), and MeOH (2 × 10 mL). The solid was then dissolved in $CHCl_3$ (5 mL) and a minimum amount of silica gel was added to adsorb the material. After the solvent was removed under reduced pressure, the dried silica gel was added to the top of a hexane-packed silica gel column, and the column was eluted with $CHCl_3$ to give **M2** as a red solid (0.58 g, 97%). ^{1}H NMR (500 MHz, $CDCl_3$): δ 8.76 (d, J = 8.0 Hz, 2H), 8.71−8.66 (m, 6H), 8.17 (d, J = 2.0 Hz, 2H), 7.72 (d, J = 6.5 Hz, 2H), 7.61 (d, J = 6.5 Hz, 2H), 7.53 (dd, J_1 = 9.0 Hz, J_2 = 2.0 Hz, 2H), 7.42 (dd, J = 9.0 Hz, 2H), 5.20 (m, 1H), 2.27 (m, 2H), 1.86 (m, 2H), 1.29−1.21 (m, 36H), 0.84 (t, J = 7.0 Hz, 6H). ^{13}C{^{1}H} NMR (125 MHz, $CDCl_3$): δ 164.7, 163.7, 163.6, 139.8, 137.2, 135.3, 135.0, 134.1, 134.0, 131.8, 131.2, 129.9, 129.7, 129.6, 127.5, 126.6, 126.3, 124.6, 124.4, 123.8, 123.7, 1231.5, 123.4, 123.1, 113.6, 112.1, 32.7, 32.4, 30.1(3 close peaks), 29.8, 27.5, 23.2, 14.4 (The observation of three carbonyl carbon resonances and one more aromatic carbon peaks is consistent with previous work on perylene bis(dicarboxyimide)s using similar swallow-tailed *N*-substituents and has been attributed to restricted rotation about the N−C_{alkyl} bonds.[70] Three alkyl carbons were not observed, $C_{65}H_{66}Br_2N_3O_4$ presumably because of overlap). HRMS (MALDI) calcd for $C_{65}H_{66}Br_2N_3O_4$ (MH^+): 1110.34, found: 1110.36. Anal. Calcd for $C_{65}H_{65}Br_2N_3O_4$: C, 70.20; H, 5.89; N, 3.78. Found: C, 70.30; H, 6.03; N, 3.76.

P1. 2,2′-(9,9-Dioctyl-9*H*-fluorene-2,7-diyl)bis(1,3,2-dioxaborinane) (0.234 g, 0.418 mmol), **M1** (0.465 g, 0.418 mmol), Aliquat 336 (40 mg), and $Pd(PPh_3)_4$ (4.8 mg, 0.0040 mmol) were charged to a 25 mL two-neck round-bottomed flask with a condenser. The system was then evacuated and refilled with N_2 four times. Toluene (5.0 mL) and 2 N aqueous K_2CO_3 (3.0 mL) were added before the mixture was heated to 90 °C and kept at that temperature for 3 d. Then, 2,2′-(9,9-dioctyl-9*H*-fluorene-2,7-diyl)bis(1,3,2-dioxaborinane) (100 mg, 0.17 mmol) in toluene (1.0 mL) was added, and the mixture was stirred for another 12 h. Iodobenzene (0.3 mL) was then added to end-cap the polymer, and the mixture was kept stirring for another 12 h. After the mixture was cooled to room temperature, it was added dropwise to 125 mL of MeOH. The resultant solid was filtered and washed with water and MeOH before drying under vacuum. The solid was washed sequentially with hot MeOH and hot acetone using a Soxhlet apparatus. The residue was then extracted with $CHCl_3$ in a Soxhlet apparatus. Most of the solvent was then removed, and the residue was passed through a short silica plug, eluting with $CHCl_3/Et_3N$ (100:1). The solvent was then removed, and the residue was dissolved in 5 mL of $CHCl_3$ and added dropwise to 100 mL of MeOH. The resulting solid was filtered and washed with water and MeOH before drying under vacuum. The precipitation procedure was repeated, and the resulting solid was then filtered and dried under vacuum to give **P1** as a red solid (0.45 g, 83%). ^{1}H NMR (500 MHz, $CDCl_3$): δ 9.0−7.0 (m,b, 24nH), 5.18 (br s, 1nH), 2.5−0.1 (m, 80nH). Anal. Calcd for polymer $(C_{94}H_{105}N_3O_4)_n$: C, 84.07; H, 8.03; N, 3.13; Found: C, 83.38; H, 7.80; N, 3.09.

P2. 2,2′-(9,9-Dioctyl-9*H*-fluorene-2,7-diyl)bis(1,3,2-dioxaborinane) (0.234 g, 0.419 mmol), **M2**(0.465 g, 0.419 mmol), Aliquat 336 (40 mg), and $Pd(PPh_3)_4$ (4.8 mg, 0.0040 mmol) were charged to a 25 mL two-neck round-bottomed flask with a condenser. The system was then evacuated and refilled with nitrogen 4 times. Toluene (5.0 mL) and 2 N aqueous K_2CO_3 (3.0 mL) were added before the mixture was heated to 90 °C and kept at that temperature for 3 d. Then 2,2′-(9,9-dioctyl-9*H*-fluorene-2,7-diyl)bis(1,3,2-dioxaborinane) (100 mg, 0.17 mmol) in toluene (1.0 mL) was added, and the mixture was stirred for another 12 h. Iodobenzene (0.5 mL) was then added to end-cap the polymer, and the mixture was kept stirring for another 12 h. After the mixture was cooled to room temperature, it was added dropwise to 125 mL of MeOH. The resulting solid was filtered and washed with water and MeOH before drying under vacuum. The solid was washed sequentially with hot MeOH and hot acetone hot acetone using a Soxhlet apparatus. The residue was then extracted with $CHCl_3$ in a Soxhlet apparatus. Most of the solvent was then removed, and the residual was run through a short silica plug, eluting with $CHCl_3/Et_3N$ (100: 1). The solvent was then removed, and the residue was dissolved in $CHCl_3$ (5 mL) and added dropwise to 100 mL of MeOH. The resulting solid was filtered and washed with water and MeOH before drying under vacuum. The precipitation procedure was repeated, and the resulting solid was then filtered and dried under vacuum to give **P2** as a red solid (0.14 g, 26%) ^{1}H NMR (500 MHz, $CDCl_3$): δ 9.0−7.5 (br m, 24nH), 5.18 (br s, 1nH), 2.3−1.0 (m, 68nH), 1.0−0.1 (m, 12nH). Anal. Calcd for polymer $(C_{94}H_{105}N_3O_4)_n$: C, 84.07; H, 8.03; N, 3.13; Found: C, 84.09; H, 7.98; N, 2.90.

2,7-Dibromo-9-dodecyl-9*H*-carbazole:[49] A mixture of 2,7-dibromo-9*H*-carbazole[53] (7.8 g, 24 mmol), 1-bromododecane (12.5 g, 50 mmol), and NaOH (2.0 g, 50 mmol) in *N,N*-

dx.doi.org/10.1021/jp3006712 | J. Phys. Chem. A 2012, 116, 4305−4317

dimethylformamide, DMF, (anhydrous, 50 mL) was stirred overnight under N_2. After the reaction, the mixture was poured into water (200 mL). Ethyl acetate (2 × 100 mL) was used to extract the product. The ethyl acetate solution was washed with water (2 × 100 mL) and saturated aqueous NaCl (200 mL), dried with $MgSO_4$, and evaporated to dryness in vacuo. The residue was recrystallized in 100 mL of ethanol to give 2,7-dibromo-9-dodecyl-9*H*-carbazole as colorless needle crystals (9.9 g, 84%). ^{1}H NMR (400 MHz, $CDCl_3$): δ 7.83 (d, J = 7.6 Hz, 2H), 7.49 (d, J = 2.0 Hz, 2H), 7.31 (dd,, J_1 = 7.6 Hz, J_1 = 2.0 Hz, 2H), 4.13 (t, J = 7.2 Hz, 2H), 1.81 (quintet, J = 7.2 Hz, 2H), 1.18−1.40 (m, 18H), 0.88 (t,, J = 7.2 Hz, 3H). The ^{1}H NMR spectrum of this compound is consistent with that reported in the literature.

3,6-Dibromo-9-dodecyl-9*H*-carbazole:[54] A mixture of 3,6-dibromo-9*H*-carbazole (7.8 g, 24 mmol), 1-bromododecane (12.5 g, 50 mmol), and NaOH (2.0 g, 50 mmol) in DMF (anhydrous, 50 mL) was stirred overnight under N_2. After the reaction, the mixture was poured into water (200 mL). Ethyl acetate (2 × 100 mL) was used to extract the product. The ethyl acetate solution was washed with water (2 × 100 mL) and saturated aqueous NaCl (200 mL), dried with $MgSO_4$, and evaporated to dryness in vacuo. The residue was recrystallized from ethanol (100 mL) to give 3,6-dibromo-9-dodecyl-9*H*-carbazole as colorless needle crystals (10.1 g, 85%). ^{1}H NMR (400 MHz, $CDCl_3$): δ 8.08 (d, J = 2.0 Hz, 2H), 7.52 (d, J = 2.0 Hz, 2H), 7.31 (d, J = 8.8 Hz, 2H), 4.18 (t, J = 7.2 Hz, 2H), 1.80 (quintet, J = 7.2 Hz, 2H), 1.18−1.44 (m, 18H), 0.86 (t,, J = 7.2 Hz, 3H). The ^{1}H NMR spectrum of this compound is consistent with that reported in the literature.

P1′. 2,2′-(9,9-Dioctyl-9*H*-fluorene-2,7-diyl)bis(1,3,2-dioxaborinane) (0.4648 g, 0.8324 mmol), 2,7-dibromo-9-dodecyl-9*H*-carbazole (0.4104 g, 0.8324 mmol), Aliquat 336 (40 mg), and $Pd(PPh_3)_4$ (9.5 mg, 0.0080 mmol) were charged to a 25 mL, two-neck, round-bottomed flask with a condenser. The system was then evacuated and refilled with N_2 four times. Toluene (8.0 mL) and 2 N aqueous K_2CO_3 (4.0 mL) were added before the mixture was heated to 90 °C and kept for 3 d. Then 2,2′-(9,9-dioctyl-9*H*-fluorene-2,7-diyl)bis(1,3,2-dioxaborinane) (100 mg, 0.17 mmol) in toluene (1.0 mL) was added, and the mixture was kept stirring for another 12 h. Iodobenzene (0.3 mL) was then added to end-cap the polymer, and the reaction was kept stirring for another 6 h. After the mixture was cooled to room temperature, it was added dropwise to 125 mL of MeOH. A formed solid was filtered and washed with water and MeOH before drying under vacuum. The solid was washed sequentially with hot MeOH and hot acetone using a Soxhlet apparatus. The residue was then extracted with $CHCl_3$ using a Soxhlet apparatus. Most of the solvent was then removed, and the residual was run through a short silica plug, eluting with $CHCl_3$ and then with THF. The solvent was then removed under reduced pressure; the residue was then dissolved in 20 mL of $CHCl_3$, and the solution was added dropwise to 200 mL of MeOH. The resulting solid was filtered and washed with water and MeOH before drying under vacuum. **P1′** was then obtained as a pale yellow solid (0.41 g, 80%). ^{1}H NMR (500 MHz, $CDCl_3$) δ 8.32 (br s, 2nH), 8.0−7.6 (br m,, 10nH), 4.50 (br s, 2nH), 2.18 (br s, 4nH), 1.90 (br s, 2H), 1.6−1.0 (br m, 42nH), 0.9−0.3 (br m, 9nH). Anal. Calcd for **P1′** $(C_{53}H_{71}N)_n$: C, 88.15; H, 9.91; N, 1.94; Found: C, 88.00; H, 10.02; N, 1.87.

P2′. 2,2′-(9,9-Dioctyl-9*H*-fluorene-2,7-diyl)bis(1,3,2-dioxaborinane) (0.4650 g, 0.8327 mmol), 2,7-dibromo-9-dodecyl-9*H*-carbazole (0.4106 g, 0.8324 mmol), Aliquat 336 (40 mg), and $Pd(PPh_3)_4$ (9.5 mg, 0.0080 mmol) were charged to a 25 mL two-neck round-bottomed flask with condenser. The system was then evacuated and refilled with N_2 four times. Toluene (8.0 mL) and 2 N K_2CO_3 aqueous solution (4.0 mL) were added before the mixture was heated to 90 °C and kept at this temperature for 3 d. Then, 2,2′-(9,9-dioctyl-9*H*-fluorene-2,7-diyl)bis(1,3,2-dioxaborinane) (100 mg, 0.17 mmol) in toluene (1.0 mL) was added, and the mixture was kept stirring for another 12 h. Iodobenzene (0.3 mL) was then added to end-cap the polymer, and the mixture was kept stirring for another 12 h. After the mixture was cooled to room temperature, it was added dropwise to 125 mL of MeOH. The formed solid was filtered and washed with water and MeOH before drying under vacuum. The solid was washed sequentially with hot MeOH and hot acetone using a Soxhlet apparatus. The residue was then extracted with $CHCl_3$ in a Soxhlet apparatus. Most of the solvent was then removed, and the residue was run through a short silica plug, eluting with $CHCl_3$ and then with THF. The solvent was removed, and the residue was dissolved in 10 mL of $CHCl_3$ before precipitating in 125 mL of MeOH. The resulting solid was filtered and washed with water and MeOH before drying under vacuum. The precipitation procedure was repeated, and the resulting solid was then filtered and dried to give **P2′** as a white solid (0.34 g, 68%). ^{1}H NMR (500 MHz, $CDCl_3$): δ 8.53 (s, 2nH), 7.8−7.6 (br m, 8nH), 7.56 (br s, 2nH) 4.39 (br s, 2nH), 2.17 (br s, 4nH), 1.94 (br s, 2nH), 1.58 (br s, 2nH) 1.4−1.0 (br m, 40 nH), 0.9−0.2 (mb, 9nH). Anal. Calcd for **P2′** $(C_{53}H_{71}N)_n$: C, 88.15; H, 9.91; N, 1.94; Found: C, 87.94; H, 9.99; N, 1.90.

AUTHOR INFORMATION

Corresponding Author

*E-mail: joe.perry@chemistry.gatech.edu (J.W.P.), seth.marder@chemistry.gatech.edu (S.R.M.).

Notes

The authors declare no competing financial interest.

ACKNOWLEDGMENTS

This material is based upon work supported in part by the DARPA (through the MORPH Program, N00014-06-1-0897), the U.S. Army Research Laboratory and the U.S. Army Research Office (under Contract/Grant Number 50372-CHMUR) and the National Science Foundation (through the Science and Technology Center Program under Agreement DMR-0120967). We thank Yan-Rong Shi for assistance with some of the linear spectroscopy and Ya-Dong Zhang for synthesizing some carbazole precursors.

REFERENCES

(1) Spangler, C. W. *J. Mater. Chem.* **1999**, *9*, 2013−2022.
(2) Pawlicki, M.; Collins, H. A.; Denning, R. G.; Anderson, H. L. *Angew. Chem., Int. Ed.* **2009**, *48*, 3244−3266.
(3) Ehrlich, J. E.; Wu, X. L.; Lee, I.-Y. S.; Hu, Z.-Y.; Rockel, H.; Marder, S. R.; Perry, J. W. *Opt. Lett.* **2002**, *25*, 1843−1845.
(4) Zheng, Q.; Gupta, S. K.; He, G. S.; Tan, L.-S.; Prasad, P. N. *Adv. Funct. Mater.* **2008**, *8*, 2770−2779.
(5) Bouit, P.-A.; Wetzel, G.; Berginc, G.; Loiseaux, B.; Toupet, L.; Feneyrou, P.; Bretonniere, Y.; Kamada, K.; Maury, O.; Andraud, C. *Chem. Mater.* **2007**, *19*, 5325−5335.
(6) Perry, J. W.; Mansour, K.; Lee, I.-Y. S.; Wu, X.-L.; Bedworth, P. V.; Chen, C.-T.; Ng, D.; Marder, S. R.; Miles, P.; Wada, T.; Tian, M.; Sasabe, H. *Science* **1996**, *273*, 1533−1536.

(7) de la Torre, G.; Vaquez, P.; Agullo-Lopez, F.; Torres, T. *Chem. Rev.* **2004**, *104*, 3723−3750.
(8) Zhou, G.-J.; Wong, W.-Y. *Chem. Soc. Rev.* **2011**, *40*, 2541−2566.
(9) Zhou, G.-J.; Wong, W.-Y.; Lin, Z.; Ye, C. *Angew. Chem., Int. Ed.* **2006**, *45*, 6189−6193.
(10) Zhou, G.-J.; Wong, W.-Y.; Cui, D.; Ye, S. *Chem. Mater.* **2005**, *17*, 5209−5217.
(11) Zhou, G.-J.; Wong, W.-Y.; Poon, S.-Y.; Ye, C.; Lin, Z. *Adv. Funct. Mater.* **2009**, *19*, 531−544.
(12) Zhou, G.-J.; Wong, W.-Y.; Ye, C.; Lin, Z. *Adv. Funct. Mater.* **2007**, *17*, 963−975.
(13) Dupuis, B.; Michaut, C.; Jouanin, I.; Delaire, J.; Robin, P.; Feneyrou, P.; Dentan, V. *Chem. Phys. Lett.* **1999**, *300*, 169−176.
(14) Cha, M.; Sariciftci, N. S.; Heeger, A. J.; Hummelen, J. C.; Wudl, F. *Appl. Phys. Lett.* **1995**, *67*, 3850−3852.
(15) Chi, S.-H.; Hales, J. M.; Cozzuol, M.; Ochoa, C.; Fitzpatrick, M.; Perry, J. W. *Opt. Express* **2009**, *17*, 22062−22072.
(16) Huang, C.; Sartin, M. M.; Siegel, N.; Cozzuol, M.; Zhang, Y.-D.; Hales, J. M.; Barlow, S.; Perry, J. W.; Marder, S. R. *J. Mater. Chem.* **2011**, *21*, 16119−16128.
(17) Cravino, A.; Sariciftci, N. S. *J. Mater. Chem.* **2002**, *12*, 1931−1943.
(18) Tan, Z.; Hou, J.; He, Y.; Zhou, E.; Yang, C.; Li, Y. *Macromolecules* **2007**, *40*, 1868−1873.
(19) Koyuncu, S.; Zafer, C.; Koyuncu, F. B.; Aydin, B.; Can, M.; Sefer, E.; Ozdemir, E.; Icli, S. *J. Polym. Sci., Part A: Polym. Chem.* **2009**, *47*, 6280−6291.
(20) Yuan, M.-C.; Su, M.-H.; Chiu, M.-Y.; Wei, K.-H. *J. Polym. Sci., Part A: Polym. Chem.* **2010**, *48*, 1298−1309.
(21) Gómez, R.; Veldman, D.; Blanco, R.; Seoane, C.; Segura, J. L.; Janssen, R. A. J. *Macromolecules* **2007**, *40*, 2760−2772.
(22) Huang, C.; Barlow, S.; Marder, S. R. *J. Org. Chem.* **2011**, *76*, 2386−2407.
(23) Würthner, F. *Chem. Commun.* **2004**, 1564−1579.
(24) Zhan, X.; Tan, Z.; Domercq, B.; An, Z.; Zhang, X.; Barlow, S.; Li, Y.; Zhu, D.; Kippelen, B.; Marder, S. R. *J. Am. Chem. Soc.* **2007**, *129*, 7246−7247.
(25) Jones, B. A.; Ahrens, M. J.; Yoon, M.-H.; Facchetti, A.; Marks, T. J.; Wasielewski, M. R. *Angew. Chem., Int. Ed.* **2004**, *43*, 6363−6366.
(26) Shoaee, S.; Clarke, T. M.; Huang, C.; Barlow, S.; Marder, S. R.; Heeney, M.; McCullocha, I.; Durranta, J. R. *J. Am. Chem. Soc.* **2010**, *132*, 12919−12926.
(27) Zhan, X. W.; Facchetti, A.; Barlow, S.; Marks, T. J.; Ratner, M. A.; Wasielewski, M. R.; Marder, S. R. *Adv. Mater.* **2010**, *23*, 268−284.
(28) Jung, B. J.; Tremblay, N. J.; Yeh, M.-L.; Katz, H. E. *Chem. Mater.* **2011**, *23*, 568−582.
(29) O'Neil, M. P.; Niemczyk, M. P.; Svec, W. A.; Gosztola, D.; L.Gaines, G.; Wasielewski, M. R. *Science* **1992**, *257*, 63−65.
(30) Wasielewski, M. R. *Acc. Chem. Res.* **2009**, *42*, 1910−1921.
(31) Bullock, J. E.; Carmieli, R.; Mickley, S. M.; Vura-Weis, J.; Wasielewski, M. R. *J. Am. Chem. Soc.* **2009**, *131*, 11919−11929.
(32) Kelley, R. F.; Tauber, M. J.; Wasielewski, M. R. *J. Am. Chem. Soc.* **2006**, *128*, 4779−4791.
(33) Kelley, R. F.; Shin, W. S.; Rybtchinski, B.; Sinks, L. E.; Wasielewski, M. R. *J. Am. Chem. Soc.* **2007**, *129*, 3173−3181.
(34) Muthukumaran, K.; Loewe, R. S.; Kirmaier, C.; Hindin, E.; Schwartz, J. K.; Sazanovich, I. V.; Diers, J. R.; Bocian, D. F.; Holten, D.; Lindsey, J. S. *J. Phys. Chem. B* **2004**, *107*, 3431−3442.
(35) Kirmaier, C.; Hindin, E. K.; Schwartz, S.; Diers, J. R.; Muthukumaran, K.; Taniguchi, M.; Bocian, D. F.; Lindsey, J. S.; Holten, D. *J. Phys. Chem. B* **2003**, *107*, 3443−3454.
(36) Li, J. L.; Grimsdale, A. C. *Chem. Soc. Rev.* **2010**, *39*, 2399−2410.
(37) Blouin, N.; Leclerc, M. *Acc. Chem. Res.* **2008**, *41*, 1110−1119.
(38) Morin, J.-F.; Drolet, N.; Tao, Y.; Leclerc, M. *Chem. Mater.* **2004**, *16*, 4619−4626.
(39) Walkim, S.; Aich, B.-R.; Tao, Y.; Leclerc, M. *Polym. Rev.* **2008**, *48*, 432−462.
(40) Park, S. H.; Roy, A.; Beaupre, S.; Cho, S.; Coates, N.; Moon, J. S.; Moses, D.; Leclerc, M.; Lee, K.; Heeger, A. J. *Nat. Photonics.* **2009**, *3*, 297−302.
(41) Wong, W.-Y.; Ho, C.-L. *Coord. Chem. Rev.* **2009**, *253*, 1709−1758 , and references cited therein.
(42) Wong, W.-Y.; Liu, L.; Cui, D.; Leung, L. M.; Kwomg, C. F.; Lee, T. H.; Ng, H. F. *Macromolecules* **2005**, *38*, 4970−4976.
(43) Xu, X.; Han, B.; Chen, J.; Peng, J.; Wu, H.; Cao, Y. *Macromolecules* **2011**, *44*, 4204−4212.
(44) Qin, R.; Bo, Z. *Macromol. Rapid Commun.* **2012**, *33*, 87−91.
(45) Barea, E. M.; Zafer, C.; Gultekin, B.; Aydin, B.; Koyuncu, S.; Icli, S.; Fabrega, F.; Santiago; Bisquert, J. *J. Phys. Chem. C* **2010**, *114*, 19840−19848.
(46) Koumura, N.; Wang, Z.-S.; Mori, S.; Miyashita, M.; Suzuki, E.; Hara, K. *J. Am. Chem. Soc.* **2006**, *128*, 14256−14257.
(47) Fang, Y.-K.; Liu, C.-L.; Chen, W.-C. *J. Mater. Chem.* **2011**, *21*, 4778−4786.
(48) Li, J. L.; Dierschke, F.; Wu, J. S.; Grimsdale, A. C.; Müllen, K. *J. Mater. Chem.* **2006**, *16*, 96−100.
(49) Iraqi, A.; Wataru, I. *Chem. Mater.* **2004**, *16*, 442−448.
(50) Ranger, M.; Rondeau, D.; Leclerc, M. *Macromolecules* **1997**, *30*, 7686−7691.
(51) Liu, B.; Yu, W.-L.; Lai, Y.-H.; Huang, W. *Chem. Mater.* **2001**, *13*, 1984−1991.
(52) Tauber, M. J.; Kelley, R. F.; Giaimo, J. M.; Rybtchinski, B.; Wasielewski, M. R. *J. Am. Chem. Soc.* **2006**, *128*, 1782−1783.
(53) Jian, H.; Tour, J. M. *J. Org. Chem.* **2003**, *68*, 5901−5103.
(54) Iraqi, A.; Wataru, I. *J. Polym. Sci. Part A: Polym. Chem.* **2004**, *42*, 6041−6051.
(55) Yu, W. L.; Pei, J.; Huang, W.; Heeger, A. J. *Adv. Mater.* **2000**, *12*, 828−831.
(56) Würthner, F.; Thalacker, C.; Diele, S.; Tschierske, C. *Chem.—Eur. J.* **2001**, *7*, 2245−2253.
(57) Beckers, E. H. A.; Meskers, S. C. J.; Schenning, A. P. H. J.; Chen, Z.; Würthner, F.; Marsal, P.; Beljonne, D.; Cornil, J.; Janssen, R. A. J. *J. Am. Chem. Soc.* **2006**, *128*, 649−657.
(58) Lindner, S. M.; Huttner, S.; Chiche, A.; Thelakkat, M. G.; Krausch, A. *Angew. Chem., Int. Ed.* **2006**, *45*, 3364−3368.
(59) Neuteboom, E. E.; Meskers, S. C. J.; Meijer, E. W.; Janssen, E. A. J. *Macromol. Chem. Phys.* **2004**, *205*, 217−222.
(60) Huang, C. Ph.D. Thesis, Georgia Institute of Technology, Atlanta, Georgia, 2010.
(61) Odom, S. A.; Lancaster, K.; Beverina, L.; Lefler, K. M.; Thompson, N. J.; Coropceanu, V.; Brédas, J.-L.; Marder, S. R.; Barlow, S. *Chem.—Eur. J.* **2007**, *13*, 9637−9646.
(62) An, Z. S.; Odom, S. A.; Kelley, R. F.; Huang, C.; Zhang, X.; Barlow, S.; Padilha, L. A.; Fu, J.; Webster, S.; Hagan, D. J.; Van Stryland, E. W.; Wasielewski, M. R.; Marder, S. R. *J. Phys. Chem. A* **2009**, *113*, 5585−5593.
(63) Ford, W. E.; Hiratsuka, H.; Kamat, P. V. *J. Phys. Chem.* **1989**, 6692−6696.
(64) Rehm, D.; Weller, A. *Isr. J. Chem.* **1970**, *8*, 258−262.
(65) Fisher, W. G.; Wachter, E. A.; Lytle, F. E.; Armas, M. *Appl. Spectrosc.* **1998**, *52*, 536−545.
(66) Xu, C.; Webb, W. W. *J. Opt. Soc. Am. B* **1996**, *13*, 481−491.
(67) Belfield, K. D.; Bondar, M. V.; Hernandez, F. E.; Przhonska, O. V. *J. Phys. Chem. C* **2008**, *112*, 5618−5622.
(68) Rumi, M.; Ehrlich, J. E.; Heikal, A. A.; Perry, J. W.; Barlow, S.; Hu, Z.; McCord-Maughon, D.; Parker, T. C.; Rockel, H.; Thayumanavan, S.; Marder, S. R.; Beljonne, D.; Brédas, J.-L. *J. Am. Chem. Soc.* **2000**, *122*, 9500−9510.
(69) Kennedy, S. M.; Lytle, F. E. *Anal. Chem.* **1986**, *58*, 2643−2647.
(70) Wescott, L. D.; Mattern, D. L. *J. Org. Chem.* **2003**, *68*, 10058−10066.